Enforced Acceleration Control for DC Actuated Rescue Robot

M.Branesh Pillai, Sakol Nakdhamabhorn, Korn Borvorntanajanya, Jackrit Suthakorn

***Abstract* -- Rescue robot robust motion control is a complex and challenging task. In general DC motor actuated rescue robot motion is defined in terms of position/velocity and forces/torque. In the rescue operation, searching for victims is an important procedure at the start of activities in support. Therefore, rescue robots must have the capability for higher mobile environment as dangerous as the ground is uneven or wet mud. In rescue robot motion control system, the task of a controller is to enforce the preferred acceleration by inserting supplementary force/torque onto the system input, thus the fusion of the preferred system acceleration is one of the essential issues in design. In this paper a novel enforced acceleration control (EAC) method is proposed to make the rescue robot acceleration response equal to the desired acceleration. During the rescue operations, the locomotion of the rescue robot's acceleration varies frequently due to the non-uniform /terrain surface. Disturbance Observer (DOB) is used to estimate and compensate the disturbance torque. To achieve the robust acceleration control for the rescue robot during the unstable acceleration period, the DOB should be tuned with the real time system parameters. Modified advanced disturbance observer (ADOB) estimate and compensate the change of system parameters. The validity and the applicability of the proposed method were proven by conducting experiments on BART LAB rescue robot in the experimental arena.**

***Index Terms*-- Advanced DOB, BART LAB rescue robot, control parameters, disturbance observer, enforced acceleration control, motion control.**

I. Introduction

RESCUE robot can be employed in disaster area for victim searching and gathering path information to rescue team in order to optimize the search and rescue plan. Recently, the natural disasters that lead to the flood by the earthquake and the global warming due to carbon dioxide are happened frequently. An example of a deadly natural calamity was the Great Chilean Earthquake, which took place in Spain in May 1960; approximately 5,000 people died from both earthquake and resulting Tsunamis. In May 2008 more than 50,000 Chinese citizens lost their lives, and over 20,000 people were missing as a result of the enormous devastative earthquake in Sichuan. Man-made disasters are also an important motivation, such as the terrible incident happening in USA on 11 September 2001 (9/11).

Most victims in 9/11 died due to the delay of aid. In such conditions, the victims' locations and conditions were difficult to conclude by rescue crews. Several researchers and academic staffs, consequently, have paid more interest in conducting research to develop rough terrain robots, especially for rescue missions. Such rescue robots are able to perform their tasks in high-risk and dangerous places such as uneven ground or wet mud [1]. The robots are able to supply images of the environment and specify victims' locations to the robot operators at the control base outside the wrecked area. In our rescue robot research, the design and development as, shown in Fig. 1 are based on the DC servo motors as their actuators (such as, presented in [2].) However, they are not so robust enough in motion control applications. This paper proposes a new practical design tool for the rescue robot robust motion control.

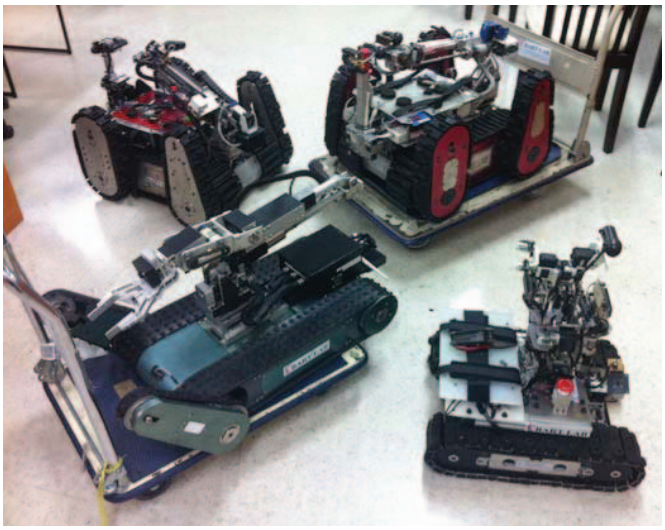

Fig. 1. Rescue robots which are actuated based on using DC motors

In rescue robots, DC servo motors have been generally used due to their trouble-free structure, outstanding control performance and economical. The performance of the rescue robotics application systems are mainly based on position and force/ torque control [3]. DC servo motors used for control applications should incorporate accurate control methodologies to obtain the desired response.

This research is partially supported by the National Research University Grant and Mahidol University, Thailand.

M.Branesh Pillai is a Ph.D. student with the Center for Biomedical and Robotics Technology (BART LAB) and Department of Biomedical Engineering, Faculty of Engineering, Mahidol University, Salaya, Nakorn Pathom 73170, Thailand (phone: +662-889-2138 ext. 6446; fax: +662-441-4250; e-mail: branesh@bartlab.org).

Sakol Nakdhamabhorn is a Ph.D. candidate with the Center for Biomedical and Robotics Technology (BART LAB) and Department of Biomedical Engineering, Faculty of Engineering, Mahidol University, Salaya, Nakorn Pathom 73170, Thailand (phone: +662-889-2138 ext. 6446; fax: +662-441-4250; e-mail: sakol@bartlab.org).

Korn Borvorntanajanya is a Master student with the Center for Biomedical and Robotics Technology (BART LAB) and Department of Biomedical Engineering, Faculty of Engineering, Mahidol University, Salaya, Nakorn Pathom 73170, Thailand (phone: +662-889-2138 ext. 6446; fax: +662-441-4250; e-mail: Korn.bov@student.mahidol.ac.th).

Jackrit Suthakorn, Ph.D. (Corresponding Author) is with the Center for Biomedical and Robotics Technology (BART LAB) and the Department of Biomedical Engineering, Faculty of Engineering, Mahidol University, Salaya, Nakorn Pathom 73170, Thailand (phone: +662-441-4255; fax: +662-441-4254; e-mail: jackrit.sut@mahidol.ac.th).

978-1-5090-2538-1/16/$31.00 ©2016 IEEE

A universal requirement for a control system is to have a robust behavior – It causes an error control as close as possible to zero in the presence of changes in actuators and/or interaction with other systems. Generally, rescue robot rotary motion uses to change both the position and the orientation due to unstable acceleration period. In this paper a novel enforced acceleration control (EAC) method is introduced to make the system acceleration equal to the desired acceleration. The control tasks will be distinct to tolerate straightforward and direct usage of Lyapunov stability criteria as an initial point in selecting the control system structure [4] [5]. In the DC motor actuated rescue robot the system robustness can be attained by considering both the position and torque/force control objective which is defined in the conditions of acceleration only. Controller parameters in such applications have to be tuned properly to obtain the desired response of the system [14].

In this paper, the torque coefficient *Kt* (0.234) of the PMDC motors used as robot wheels was measured by using the laboratory DC motor rotor stall test [6]. The friction parameters (*Tf* and *Bω*) the static friction *Tf* is the force required to start the motion from the stand still status. When the motor starts to rotate, viscous friction *Bω* appears and it increases with the increase of velocity. Both the frictional components *Tf* (0.86N) and *B (*0.035) are identified by conducting the continual velocity motion test [6], and the DOB are used as a torque sensor. DOB identifies the total mechanical load and the effect of system parameters change which reflects as the total disturbance of the DC motor [7-9][12]. However, when the rescue robot is in operation, mechanical parameters (torque coefficient *Kt*, moment of inertia *J*) and friction components are exposed to be changed [14].

In this paper the advanced disturbance observer (ADOB) is introduced to estimate and eliminate the change of real time motor inertia (actual inertia) of the rescue robot during unstable acceleration period. ADOB control tool is much simpler and easy to use compared to conventional methods [13]. The torque sensation, sensed through the torque sensors are often dull due to narrow bandwidths of torque sensors. Therefore, the authors interested to use Disturbance Observer (DOB) as the torque sensor [10]. ADOB based real time change of inertia estimation and compensation methodology is explained in the modeling section.

In the proposed enforced acceleration control (EAC), the preferred acceleration is imposed due to the supposition of change of system parameters and also the overall external disturbance effect. ADOB is incorporated with the proposed EAC in the controller itself to estimate and compensate the system nonlinearities in terms of parameters, is explained in the modeling section.

The validity and the applicability of the ADOB were proven by conducting experiments using various types of external disturbances applied towards wheels (DC Motors) of the BART LAB rescue robot [2] and the applicability of the enforced acceleration control were proven by conducting experiments on BART LAB rescue robot in different experimental arena.

This paper is organized as follows. In Section 2, DC motor and the disturbance observer modeling are explained. Further, in this section, the introduced new advance disturbance observer as ADOB to calculate the motor inertia and novel Enforced Acceleration Control (EAC) method is also explained. This is the main significant addition of this research. Then, the validity and the applicability of the proposed control system were analyzed experimentally and the results are discussed in Section 3. Finally, this paper is summarized in Section 4.

II. SYSTEM MODELLING

A. DC Motor Modelling

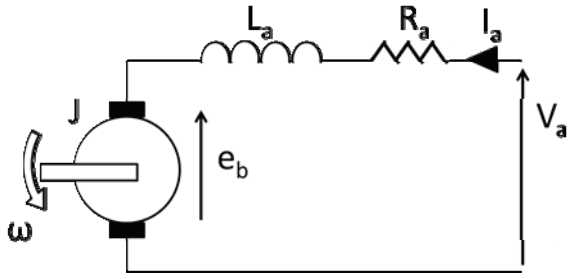

Fig. 2. Electrical model of a DC motor

Applying Kirchoff's voltage law to the above circuit Fig. 2.with armature resistance R_a, armature inductance L_a, armature current I_a, torque coefficient K_t, moment of inertia of motor J, back emf constant K_e and armature voltage V_a.

$$V_a = L\frac{dI_a}{dt} + RI_a + e_b \tag{1}$$

The back emf e_b is generated by the angular speed ω and given by the expression below.

$$e_b = K_e\omega \tag{2}$$

Motor torque T_m is proportional to armature current I_a.

$$T_m = K_t I_a \tag{3}$$

Motor torque T_m with the presence of load torque T_l can be expressed as follows. Where, T_{sf} is the static friction torque and B is the viscous friction coefficient.

$$T_m = J\frac{d\omega}{dt} + T_{sf} + B\omega + T_l \tag{4}$$

Equations (1)-(4) can be represented by the block diagram as shown below Fig.3 (a), for further analysis. From (5) and (6), the block diagram of a servo motor can be modeled as shown below Fig.3 (b). T_{dis} consists of load torque T_l, and torque due to fixed friction T_{sf} and viscous friction $B\omega$. Equation (4) can be re-written as follows. Where, T_{dis} represents all the disturbances and the load torque.

$$J\dot{\omega} = T_m - T_L \tag{5}$$

$$J\dot{\omega} = K_t I_a - T_L \tag{6}$$

$$T_{dis} = T_l + T_{sf} + B\omega \tag{7}$$

Usually the armature current I_a is controlled by PWM based voltage controller [15], [9]. When the disturbance torque is present, the motor does not provide the desired output. To guarantee the expected functionalities of the motor, it is important to compensate the disturbance torque. Disturbance Observer is used here to measure the

disturbance torque and compensate it to the system [3] [16].

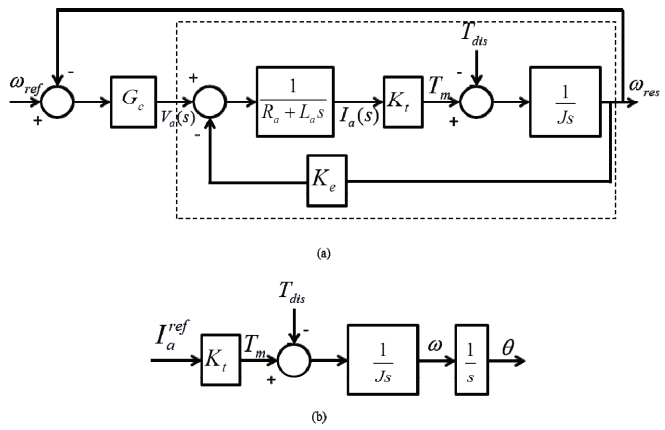

Fig. 3. (a) Block diagram of DC motor. (b) Control block diagram of servo motor

B. Disturbance Observer Modeling

The inertia of the DC motor J can be changed due to the mechanical configuration of the motion system. The torque coefficient K_t also varies according to the rotor position of the electric motor due to irregular distribution of magnetic flux on the surface of rotor [11][12]. If the nominal motor inertia J_n varies by σJ and nominal torque coefficient K_{tn} varies by σK_t, the actual J and K_t can be represented by (8) and (9) respectively, as shown in Fig.4.

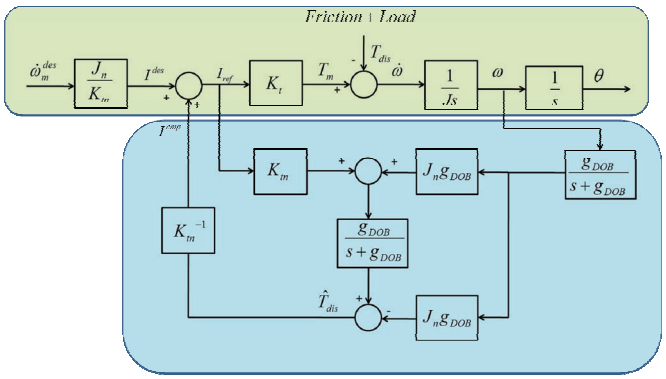

Fig. 4. Control block diagram of Disturbance observer

$$J = J_n + \sigma J \tag{8}$$

$$K_t = K_{tn} + \sigma K_t \tag{9}$$

From (6), (7), (8) and (9), it can be determined that

$$T_{dis} = K_{tn} I_a - J_n \dot{\omega} \tag{10}$$

Disturbance torque T_{dis} consists of load torque, frictional torques and torques arising from the parameter variations.

$$T_{dis} = T_l + T_{sf} + B\omega + \sigma J\dot{\omega} - \sigma K_t I_a \tag{11}$$

T_{dis} can be calculated from the right hand side known parameters of (10). $\hat{T}_{dis}$ is the estimated disturbance torque which is the output of the disturbance observer in Fig. 4 and g_{DOB} is the cut-off frequency of the observer. The control accuracy is further improved by considering the disturbance observer errors. The system parameters like *Kt, J, B*, and T_{sf} have to be accurate for an effective compensation. Compensation happens after one program cycle. The sampling time used for this experiment is 80 µs and it makes the DOB to compensate fast. An optimum cut-off frequency is selected for the maximum effectiveness, and the system is considered as a second order system due to the small DC motor with high torque used here.

C. Advance Disturbance Observer Modeling

Disturbance observer can be used for many applications such as to estimate the change of motor inertia with some advanced modifications. For example, the disturbance observer can be used to estimate the torque variation which generates due to the change of moment of inertia. This estimation is done without using any torque sensor and only by identifying the internal disturbance of the system [17] [18]. Disturbance observer output $\hat{T}_{dis}$ is calculated using the known parameters of (10). In this step, a low pass filter with disturbance gain g_{DOB} is used to suppress noise components adding by differentiation block $J_n g_{DOB}$. Load torque, frictional torque and torque due to motor constant variation are removed from the DOB output. Thus, the DOB output consists of only the torque components arising due to moment of inertia variation. Fig.5 represents the advance version of the DOB.

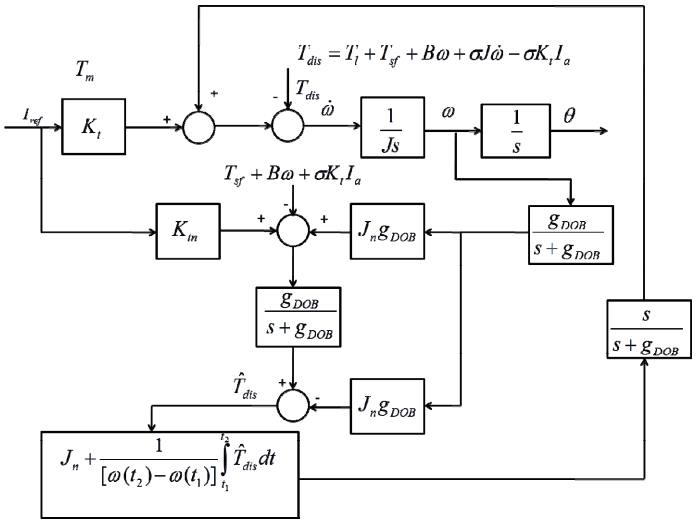

Fig. 5. Control block diagram of advance disturbance observer

In this research, the friction components T_f (0.86N) and (B=0.035) are identified by conducting the continual velocity motion test [6]. If a large size DC motors are used (>200W), the friction components can be separately calculated and compensated to the system [15] [19] [20]. By eliminating the pre estimated parameters value from the DOB output inside the controller itself then, the advanced disturbance observer output represents only the estimated change of inertia of the motor σJ. This tool can be effectively used to find the real inertia value of any control system incorporates DC motor. The σJ variation can be added or subtracted from the nominal motor inertia and it is possible to fine tune the system by analyzing the torque response graphs as shown in Fig. 6 for positive and negative σJ values respectively. The dotted red lines in Fig. 6 represent the torque variation when the applied motor inertia value equals to the actual value. In this process, the motor is accelerated from zero to a constant velocity.

The acceleration is kept constant over the accelerating period. The torque response of this test can be further

elaborated with the aid of Fig. 6 and which is graphical explanation for (11). The deviation of moment of inertia from the nominal moment of inertia is the gap between red dotted line and the waveform acceleration period of the Fig. 6.

$$\hat{T}_{dis} = \sigma J\dot{\omega} \tag{12}$$

By combining (8) and (12), $\hat{T}_{dis}$ can be expressed in (13).

$$\hat{T}_{dis} = (J - J_n)\dot{\omega} \tag{13}$$

$$\int_{t_1}^{t_2} \hat{T}_{dis}dt = (J - J_n)[\omega(t_2) - \omega(t_1)] \tag{14}$$

$$J = J_n + \frac{1}{[\omega(t_2) - \omega(t_1)]}\int_{t_1}^{t_2} \hat{T}_{dis}dt \tag{15}$$

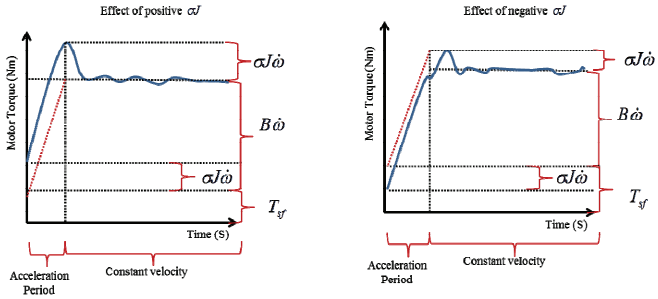

Fig. 6. Torque response for positive and negative σJ

Then in (14) the expression is integrated for the time interval t_1 to t_2 of executed controller program cycle. Motor inertia J can be calculated from the right hand side known parameters of (15) and add it to the inner loop of the motor itself.

D. *Enforced acceleration control*

The dynamics of the feedback system are determined by the proper selection of system convergence [4]. If asymptotic convergence is imposed then the generalized error reaches stability $e(k) = 0$ as time lean towards to infinity. The feedback system dynamics are well explained by the convergences law $\dot{e}(k) + ke(k) = 0$. Equation (10) explains that the acceleration or torque of the system depends on the choice of feedback system's control input. In our control design as per (16) the desired acceleration $\dot{\omega}_{des}$ is selected as the total additional value of the convergence acceleration $\dot{\omega}_{con}$ and the equivalent acceleration $\dot{\omega}_{eq}$.

$$\dot{\omega}_{des} = sat[\dot{\omega}_{eq} + \dot{\omega}_{con}] \tag{16}$$

From the known control output /input and the generalized error $e(k)$ equivalent acceleration can be derived in real time. By using the desired convergence law, convergence acceleration can be specified. The saturation function in (16) shows the control input is bounded, so that the desired motion can be achieved in the bounded domain within the system state space. A uniqueness of the system deceits in the structure of the control block computing the control error. In this control structure, $e(k)$ is the control variable.

The control output is then imposed by quality of the stability solution and by choice of the reference selected. Convergence acceleration is the most precise term of the control. The role of the convergence acceleration is to impose the required convergence rate and the solution to system stability. In position control both position and velocity feedback are mandatory to assure the convergence and system stability. The convergence acceleration can be chosen proportional to control error when the control tasks that depend on system's velocity and the convergence acceleration must be chosen as a function of the control error and its derivative when the control tasks not depends on system's velocity.

In the proposed control, as shown in Fig.7 these differences are determined by choosing a control structure of the generalized error $e(k)$ to include the velocity. Here, the required acceleration is imposed due to the advance disturbance observer were the inertia and the disturbance are exactly known, thus selection of torque as in (12) essentially stands for required acceleration controller. In this paper the control output was a defined function of position, velocity and acceleration and the generalized equation is given as (17) in which G_c is the system gain and it should not be zero.

$$\dot{e}(k) = G_c(\dot{\omega}_{des} - \dot{\omega}_{eq}) \tag{17}$$

The motor torque that imposes the required acceleration (16) and (17) in the system as shown in (10) can be written as (18).

$$T_m = sat\{T_{dis} + a(n)[\dot{\omega}_{eq} + \dot{\omega}_{con}]\} \tag{18}$$

Were $a(n)[\dot{\omega}_{eq} + \dot{\omega}_{con}]$ denotes the required acceleration and $a(n) = [J_n + \sigma J]$. The disturbance effect is added to the required acceleration (16) as a compensation to make the system acceleration to the preferred acceleration.

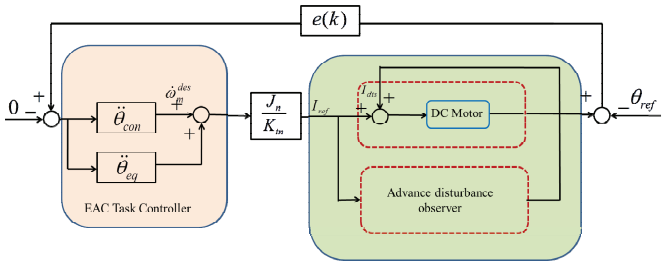

Fig. 7. Proposed enforced acceleration control structure

The input motor torque as in (18) stands for the proposed enforced acceleration controller of the rescue robot. Where the essential acceleration imposes the acceleration tracking, which means the disturbance effect on the non-uniform acceleration period and especially in this research change of motor inertia (σJ) was considered throughout. In the rescue robot precise control, system disturbance is a considerable property of the control design and torque due to interactions with environments. Proposed enforced acceleration control structure shown in Fig.7, the required acceleration is determined in the outer control loop when the task is dependent and the disturbance compensation taken place in the inner control loop itself

A control module for Fig. 7 is modeled in the Matlab Simulink environment, and the frequency responses are analyzed for position response by changing the inertia value of the motor from 0.24 – 0.94 kg cm^2 with different cutoff

frequencies. This simulation was carried out to identify the effect of the changing motor inertia of the DC motor. According the simulation results in Fig. 8, there is a significant change in the system bandwidth when the moment of inertia is changed within this considered range. Therefore, it is important to identify the exact inertia value of the DC motor to achieve the desired system response. Inability to identify the correct motor inertia will lead the system to an undesired state.

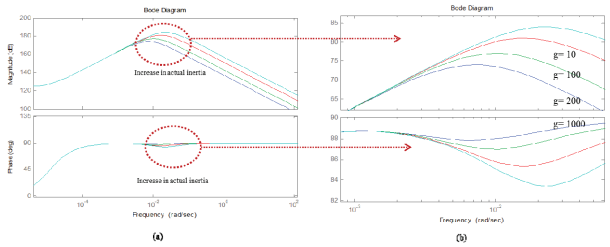

Fig. 8. Frequency response with different motor inertia values

The validity of the proposed enforced acceleration control method was proven in the experiment section. In this experiment velocity response is calculated by using position response and pseudo derivation. The reaction curve control method [21] is used as the lower level control instead of using PID control.

III. EXPERIMENTAL RESULTS AND DISCUSSION

A. *BART LAB rescue robot as experimental platform*

This section describes a BART LAB rescue robot platform, which was used in the experiment shown in Fig.9.

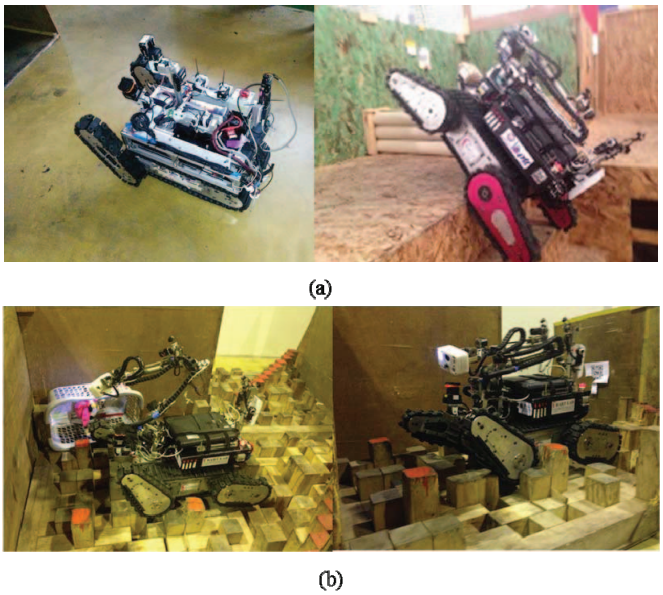

Fig. 9. BART LAB rescue robot. (a) Platform with DC servo motors. (b) Rescue robot on different type of random step field

Both ADOB and EAC control algorithms were implemented into our rescue robot platform. The rescue robot platform was driven by a tracked differential driven mechanism, and two Maxon DC motor was used to transmit power in each side of the tracked platform as a wheels. The tracked driven platform enhances robot mobility in order to move through a complex terrain as shown in Fig. 9 (b). The robot platform also consists of 2 front flippers. The flippers assists the robot to maintain its stability while climbing up and down on rough terrain, step way or stairway. The specification of the DC motor is determined by calculating the torque which is able to drive 60 kg of robot weight and overcome the friction of track wheels. Then, the robot is installed with two 24 Volt Maxon DC motor of 80 Watts power that can generate torque 3.4 N/M and maximum speed 200 RPM. The DC motor is attached with 500 resolution encoder as a velocity feedback sensor. The Allegro ACS754 current feedback sensor is integrated into the robot feedback system. The current feedback sensor primary sampled current is ±50 A with Sensitivity is 40 mV/A and the reference power supply is kept constant all through the operation.

B. *Experimental results*

In this section, experimental results of the both advance disturbance observer (ADOB) and enforced acceleration control (EAC) on BART LAB rescue robot are shown below. As shown in Fig.10, the external disturbance applied on the robot track wheels was considered as all the three disturbance modes: supporting, opposing, and periodic. In addition to considering the experiment point of view, the disturbance effects were generated in the EAC control block itself as shown in Fig. 5. In the supporting and opposing modes, the applied disturbances were generated by the controller with a constant PWM. In the periodic disturbance mode, the applied disturbance is a constant sinusoidal disturbance with varying frequencies. The directions of rotation of the actuator in each simulated disturbance modes are indicated by arrows and also the functional hardware block diagram in the Fig. 10. The experimental parameters used in the control system are shown in Table 1.

Table 1 EXPERIMENTAL PARAMETERS

Parameter	Symbol	Value	Units
Nominal Motor inertia	J_n	0.94	kgcm^2
Motor inertia	J	0.94	kgcm^2
Nominal Torque coefficient	K_{tn}	0.234	Nm/A
Torque coefficient	K_t	0.234	Nm/A
Proportional constant	K_p	80.00	--
Integral constant	K_i	0.015	--
Derivative constant	K_d	9.52	--
Cut-off frequency of low pass filter	g_{DOB}	200.0	Hz
Viscous friction coefficient	B	0.035	Nm/rpm
Static friction	T_{sf}	0.86	Nm
Current feedback gain	Y	0.01	Hz

Fig. 11 shows the change of actuator inertia of the wheels of the rescue robot, were there different types of external disturbance was applied to the main motors of the robot. In

Fig.11 the graphs shows the disturbance torque responses of the two actuators (tracking wheels) of the rescue robot estimated by ADOB. As per the (12) and (15): the graph clearly shows that the change of inertia depends on the types of external and internal disturbance effect applied to the system. Fig. 11(a) and (b) shows the ADOB responses of the system for supporting, opposing and periodic disturbances respectively.

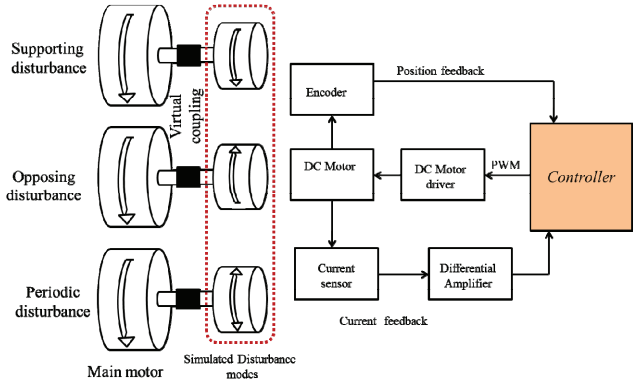

Fig. 10. Simulated disturbance modes and functional hardware block diagram

The identifiable frequency variations in the system response are caused by the feedback component of the controller. During a high frequency, known parametric supporting disturbance is applied; the ADOB compensates for it and produces a slightly oscillating response. The same system response can be identified for both opposing and periodic disturbances. When ADOB is applied for the above supporting, opposing and periodic disturbances cases, and the real-time torque response curves in Fig. 13 (a) and (b) shows the performance of accurate change of system inertia. The system responses are used in the inner loop of EAC to compensate for the change of overall system parameters. The effect of ADOB incorporated in EAC results in velocities closer to the reference velocities and almost cancelled out external disturbances.

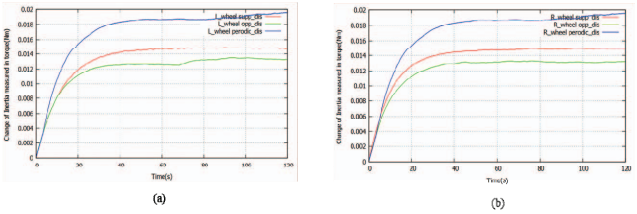

(a) (b)

Fig. 11. ADOB output for different modes of disturbances. (a) Left wheel. (b) Right wheel

To validate the proposed EAC method: the EAC control algorithm incorporated rescue robot was tested in two different types of terrain arena shown in Fig.9 (b), with a rough/dangerous step field and the smoother slope region with the reference input of 60rpm constant velocity. Fig.12 (a) and (b) represents the velocity response of the two tracked wheels of the robot when navigating in the 15degree and 30 degree smooth slope terrain surface.

Fig.13 (a) and (b) shows the velocity response of the two tracked wheels of the robot in a rough and dangerous random step field. Fig. 12 illustrates rapid velocity response variations occurring simultaneously, circled with blue color which shows that the robot tried to change the path /sometime get struck with the random step field environment. In the random step field: almost all the time the velocity response was not constant which proves that the acceleration of the track wheels was always changing with time.

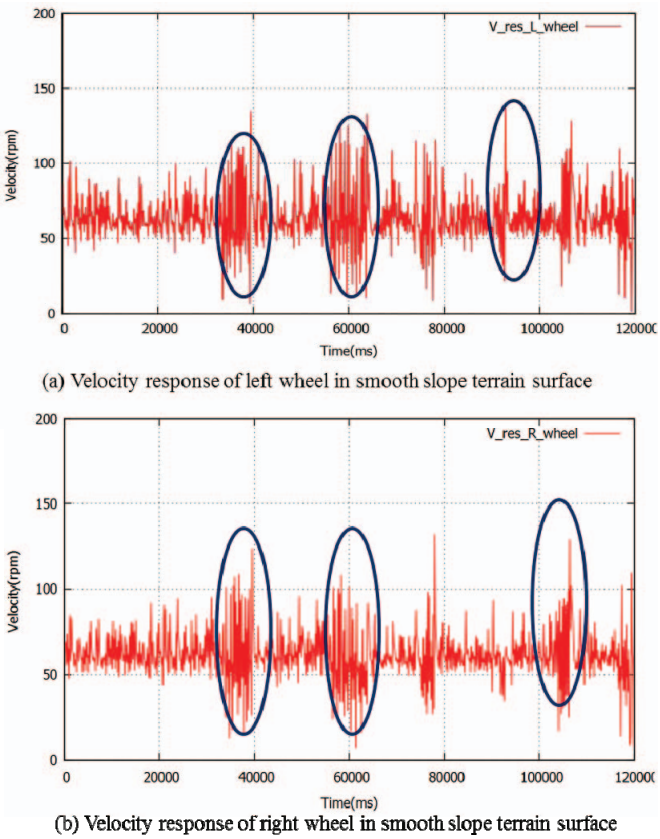

Fig. 12. Velocity response (a) Left wheel in smooth slope terrain surface. (b) Right wheel in smooth slope terrain surface.

Thus, in such case need of acceleration control is very necessary and it is important to monitor the error response also in parallel with the velocity response because the controller convergence can be tuned according to this response only, if the controller compensation does not acts as quick as fast then the system instability will occur very easily. The overall system inertia is very large because the weight of the robot is almost 60kg, in this case simple PID based controller not suits perfect, so that to overcome the system instability proposed EAC was incorporated to make the system acceleration equal to the desired acceleration.

Figure 14 (a) and (b), Fig. 15(a) and (b) shows the real time velocity error response of the robot track wheels in smooth slope terrain and random step field. In Fig.16 and 17 the graphs show the controller error output responses of the robot track wheels in smooth slope terrain and random step field correspond to with and without proposed EAC control algorithm. The applicability of the proposed method was validated by using controller error output responses with and without proposed EAC. Fig. 16 (a) and (b), Fig. 17(a) and (b) clearly shows the improved performance when the EAC is applied to the system.

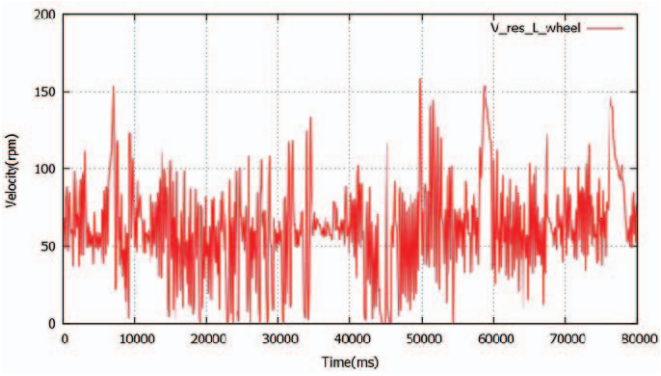

(a) Velocity response of left wheel in non uniform surface

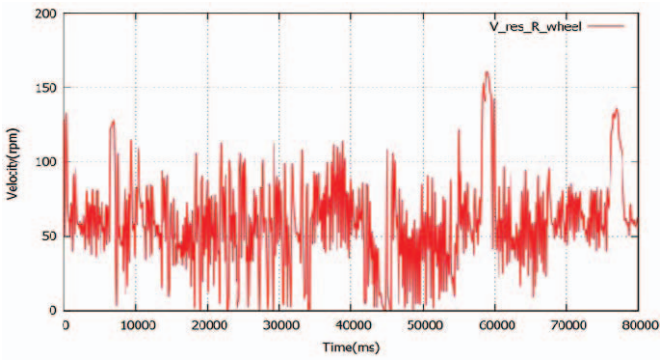

(b) Velocity response of right wheel in non uniform surface

Fig. 13. Velocity response (a) Left wheel in non-uniform surface. (b) Right wheel in non-uniform surface.

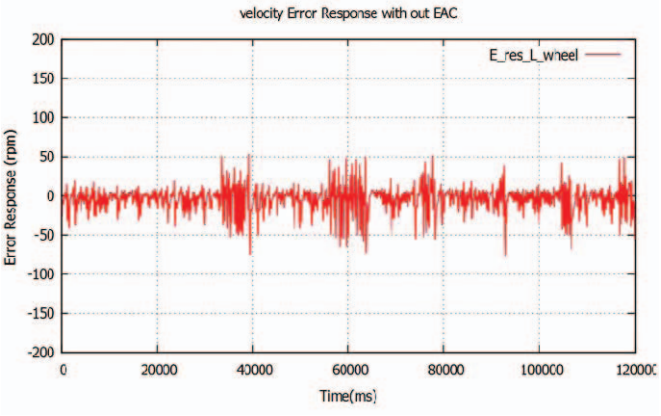

(a) Velocity error response of left wheel

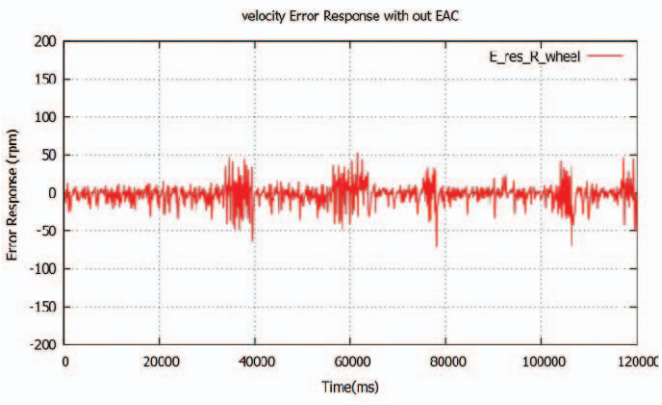

(b) Velocity error response of right wheel

Fig. 14. Velocity error response in smooth slope terrain. (a) Left wheel. (b) Right wheel

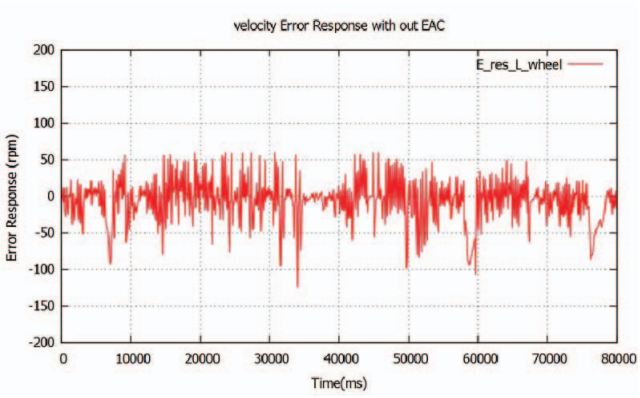

(a) Velocity error response of left wheel

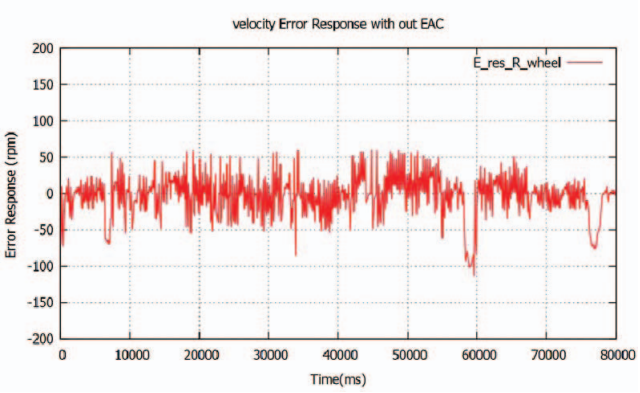

(b) Velocity error response of right wheel

Fig. 15. Velocity error response in and random step field. (a) Left wheel. (b) Right wheel.

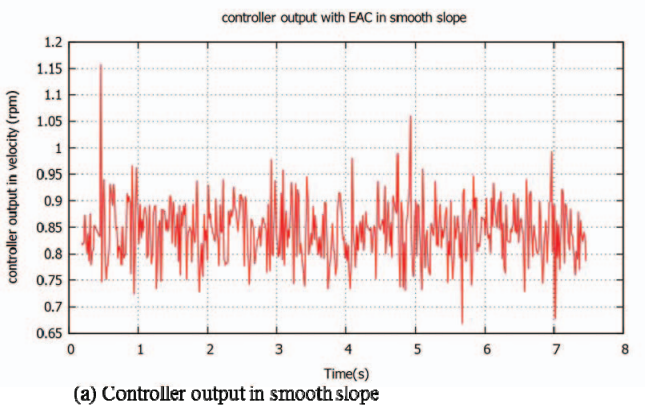

(a) Controller output in smooth slope

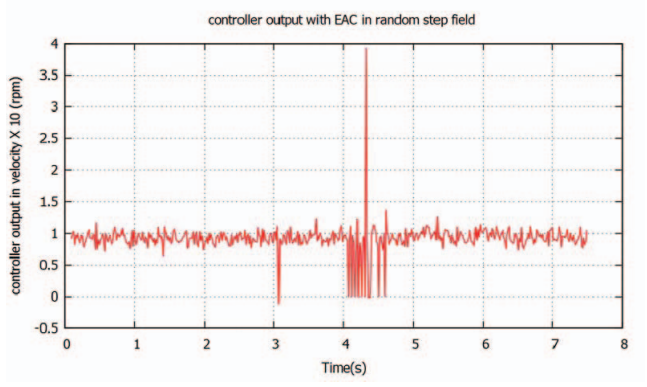

(b) Controller output in random step field

Fig. 16. Controller output with EAC. (a) Smooth slope. (b) Random step field.

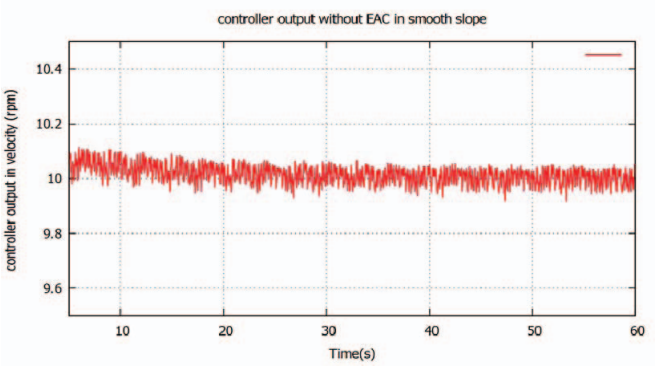

(a) Controller output in smooth slope

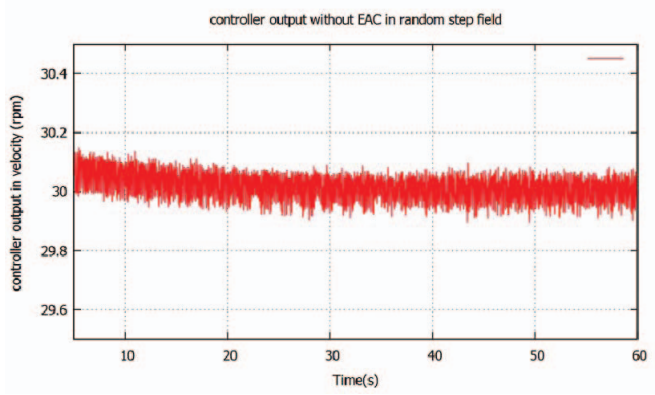

(b) Controller output in random step field

Fig. 17. Controller output without EAC. (a) Smooth slope. (b) Random step field.

IV. CONCLUSION

In this paper: we propose a novel enforced acceleration control (EAC) method to make the system acceleration equal to the desired acceleration and also the concept to estimate the change of system inertia of a DC motor used in rescue robot as tracking wheels. The stability and the frequency response of the Enforced Acceleration Control (EAC) incorporated advance disturbance observer control system (ADOB) were analyzed using control technique which shows that there is a significant change in the system bandwidth when the moment of inertia is changed within the considered range. In the proposed EAC control system, the desired acceleration is imposed due to the supposition that change of real time inertia determined by ADOB and the disturbance are precisely identified, thus election of torque as in (15) fundamentally stands for preferred acceleration controller.

The ADOB incorporated system showed a higher degree of system stability. To check the responses of the system, different types of disturbances effects were used in the experiments. In additional, these responses were examine methodically with EAC incorporated BART LAB rescue robot. The system response increases when the EAC and ADOB are incorporated to the system, where the response of the system has become extremely robust as seen in the results. When the controllers gain is increased, it results in high motor torque frequency variations. ADOB based EAC controller is more appropriate for the system with DC motors which are subjected to high disturbances and using under nonlinear conditions in uneven motion. Also, this technique can be further used for DC motor parameters estimation, non- linear components identification for precise motion control.

V. ACKNOWLEDGMENT

Authors would like to express their gratitude to BART LAB Rescue Robot team members and BART LAB Researchers for their kind support and also for assembling a BART LAB rescue robot platform to implement in this work.

VI. REFERENCES

[1] H. Okada, T. Iwamoto and K. Shibuya, "Water-Rescue Robot Vehicle with Variably Configured Segmented Wheels" *Journal of Robotics and Mechatronics,* Vol.18, No.3, 2006, pp.278-285.

[2] J. Suthakorn, S.S.H. Shah , S. Jantarajit , W. Onprasert and W. Saensupo, S. Saeung, S. Nakdhamabhorn,V. Sa-Ing, and S. Reaungamornrat, "On the Design and Development of A Rough Terrain Robot for Rescue Missions", *Proceedings of the 2008 IEEE International Conference on Robotics and Biomimetics* Bangkok, Thailand, February 21 - 26, 2009.

[3] Ohnishi, K., Shibata, M., and Murakami, T, "Motion control for advanced mechatronics," *IEEE/ASME Trans. Mechatronics,* vol.1, no.1, pp.56-67, Mar-1996.

[4] Asif Sabanovic and Kouhei Ohnishi, "Motion control systems," IEEE press John Willey and sons (Asia) pte Ltd, First Edition, 2011.

[5] Hongbing Li; Kawashima, K.; Tadano, K.; Ganguly, S.; Nakano, S., "Achieving Haptic Perception in Forceps' Manipulator Using Pneumatic Artificial Muscle," Mechatronics, IEEE/ASME Transactions on , vol.18, no.1, pp.74,85, Feb. 2013.

[6] Kobayashi, H., Katsura, S., and Ohnishi, K., "An Analysis of Parameter Variations of Disturbance Observer for Motion Control," IEEE Trans. Ind.Electron., vol. 54, no.6, pp.3413-3421, Dec-2007.

[7] Senevirathne H.R, Abeykoon A.M, Pillai M.B, Disturbance rejection analysis of a disturbance observer based velocity controller, In: 6th IEEE International Conference on Information and Automation for Sustainability, Beijing, China,2012.p.59-64.

[8] Zhang P, Bai H, Derivation of Load Model Parameters using Improved Genetic Algorithm, In:3rd International Conference on Electric utility deregulation and restructuring and Power technologies, Nanjuing, China,2008.p. 970–77.

[9] H.A.N.D.Dayarathna, L.L.G.Prabuddha, K.L.D.N.J. Ariyawansha,M.K.C.D.Chinthaka, A.M.H.S. Abeykoon, M.B.Pillai, Sensorless contact position estimation of a mobile robot in pushing motion, In:IEEE International Conference Circuits, Power and Computing Technologies,India,2013.p.344-49.

[10] A.M.Harsha S.Abeykoon and M.Branesh Pillai, "RTOS based embedded controller implementation of a bilateral control system," J.Natn.Sci.Foundation Sri Lanka 2014, 42 (3), 217-228.

[11] Funabiki, S., Fukushima, T., "Current commands for high-efficiency torque control of DC shunt motor," in *IEE Proceedings B, Electric Power Applications,* vol. 138, no. 5, pp. 227-332, Sept-1991.

[12] Abeykoon, A.M.H.S., Senevirathne, H.R., "Disturbance observer based current controller for a brushed DC motor," in *Proc. 6th IEEE Information and Automation for Sustainability* , 2012, pp. 47-52.

[13] Ohnishi, K., Katsura, S., and Shimono, T., "Motion Control for Real-World Haptics," *IEEE Trans.Ind. Electron. Magazine*, vol.4, no. 2, pp. 16-19, June 2010.

[14] C. Ganesh, B. Abhi, V. P. Anand, S. Aravind, R. Nandhini,and S. K. Patnaik, "DC Position Control System-Determination of Parameters and Significance on System Dynamics, "*ACEEE Trans. J.Electrical and Power Eng.*," vol.3, no.1, pp.1-5, Feb-2012.

[15] Kobayashi, H., Katsura, S., and Ohnishi, K., "An analysis of parameter variations of disturbance observer for haptic motion control," in Proc.

31st IEEE Annu.Conf. IECON, 2005, pp.

[16] Saito, E., and Katsura, S., "A filter design method in disturbance observer for improvement of robustness against disturbance in time delay system," in Proc. IEEE Industrial Electronics (ISIE), 2012, pp. 1650-1655.

[17] Ohba, Y., Sazawa, M., Ohishi, K., Asai, T., Majima, K., Yoshizawa, Y., and Kageyama, K., "Sensorless Force Control for Injection Molding Machine Using Reaction Torque Observer Considering Torsion Phenomenon," *IEEE Trans. Ind. Electron.*, vol. 56, no. 8, pp.2955-2960, Aug-2009.

[18] Ohba, Y., Ohishi, K., Katsura, S., Yoshizawa, Y., Kageyama, K., Majima, K., "Sensor-less force control for injection molding machine using reaction torque observer," in *Proc. IEEE ICIT,* 2008, pp.1-6.

[19] Minaki, R., Hoshino, H., and Hori, Y., "Driver steering sensitivity design using road reaction torque observer and viscous friction compensation to Active front steering," in Proc. *IEEE Industrial Electronics (ISIE)*, 2010, pp.155-160.

[20] Ito, K., Iwasaki, M., and Matsui, N.,"GA-based practical compensator design for a motion control system," *IEEE/ASME Trans.Mechatronics,* vol.6, no.2, pp.143-148, Jun-2001.

[21] S. Sen and S. Mukhopadhyay, "Industrial automation and control-Process control," NPTEL E-learning courses from the IITs and IISc, india.

VII. BIOGRAPHIES

Branesh M. Pillai received the B.E. degree in Electrical & Electronic Engineering from Anna University, India in 2007 and the M.Sc. degree in Systems & Controls Engineering from University of Moratuwa, Sri Lanka in 2013.He is currently a Ph.D. student with the Center for Biomedical and Robotics Technology (BART LAB) and Department of Biomedical Engineering, Faculty of Engineering, Mahidol University, Thailand. His research interests include control systems, bilateral control, motion control, and medical robotics control. Mr. Branesh is a student member of IEEE. He received the best paper award in IEEE ICCPCT in 2013.

Sakol Nakdhamabhorn received the B.E. degree in computer Engineering and the M.E. degree in Biomedical Engineering from Mahidol University, Nakornpathom Thailand, in 2007 and 2011, respectively. He is currently a Ph.D. candidate with the Center for Biomedical and Robotics Technology (BART LAB) and Department of Biomedical Engineering, Faculty of Engineering, Mahidol University. His research interests include medical imaging, computer assisted surgery, medical robotics, and robot control and interface.

Korn Borvorntanajanya received the B.E. degree in Biomedical Engineering from Mahidol University, Nakornpathom, Thailand. He is currently a Master degree student in Biomedical Engineering, Mahidol University. His research interests include medical imaging, medical robotics, and robot control and interface.

Dr. Jackrit Suthakorn was born in Thailand on May 24, 1973. He received the B.E. degree in mechanical engineering from Mahidol University, Bangkok, Thailand in 1995, and the Master degree in Control Engineering from the Michigan Technological University, Michigan, USA in 1998 and Ph.D. in Robotics from the Johns Hopkins University, Baltimore, Maryland, USA in 2003. He had established the Center for Biomedical and Robotics Technology (BART LAB) in 2004 which he was the Executive Director of the Center, and also had also established the Thailand's first Department of Biomedical Engineering in 2006 which he was the first Department Chair.

He is currently the Dean of Faculty of Engineering, Mahidol University. His current research interests include Robot-Assisted Surgery, Surgical Navigations, Rescue Robot and @Home Service Robot which the past research interests included Self-Replicating Robots and Binary Hyper-Redundant Robotic Manipulators.